electronics

MDPI

Article

Multi-Channel Virtual Instrument for Measuring Temperature—A Case Study

Romuald Masnicki [1,*] and Dariusz Swisulski [2]

[1] Faculty of Electrical Engineering, Gdynia Maritime University, 81-225 Gdynia, Poland
[2] Faculty of Electrical and Control Engineering, Gdansk University of Technology, 80-233 Gdansk, Poland; dariusz.swisulski@pg.edu.pl
* Correspondence: r.masnicki@we.umg.edu.pl; Tel.: +48-58-5586-490

Abstract: The article presents the hardware and software configuration of the developed multi-channel temperature measurement system as well as calibration procedures and measurement results verifying the properties of measurement channels. The system has been developed and dedicated primarily for measuring the temperature distribution in a laboratory model simulating underground power lines. With the adopted configuration of the analog part of each measurement channel, the main functions in the system developed as a virtual instrument are performed in its software. The instrument input circuits contain NTC (negative temperature coefficient) thermistors used as temperature sensors. The resistance of each of the thermistors connected in the voltage divider circuits is converted into a voltage. The obtained voltages in the measurement channels, after analog-to-digital conversion (ADC), are processed in subsequent operations in the instrument's software. In addition to the basic function of the device, which is the multi-channel temperature measurement, the operations of identifying the characteristics of the thermistors used and calibrating each of the individual measurement channels are performed. The article contains sample results of the calibration of measurement channels and temperature verification measurements used to evaluate the properties of the developed system. The obtained inaccuracy of the temperature measurement in each of the channels is less than 0.4 °C.

Keywords: multi-channel measurement system; temperature measurement; NTC thermistor; virtual instrument; measurement channel calibration

Citation: Masnicki, R.; Swisulski, D. Multi-Channel Virtual Instrument for Measuring Temperature—A Case Study. *Electronics* **2023**, *12*, 2188. https://doi.org/10.3390/electronics12102188

Academic Editors: Flavio Canavero and Nikolay Hinov

Received: 8 March 2023
Revised: 13 April 2023
Accepted: 8 May 2023
Published: 11 May 2023

1. Introduction

The configuration of modern instruments for measuring analog quantities is, in most cases, based on digital data processing systems. In the acquisition part of the measurement chain, from the input circuits, possibly with the measurement sensor, to the analog-to-digital converter (ADC), hardware processing of measurement information carried by signals takes place. Compared to traditional analog devices, in digital devices, the circuitry of the analog part of the measurement chain is reduced in order to quickly access the digital representation of the analog signal processed in the ADC [1]. In this way, the impact of various disturbances on the processed information is avoided or significantly limited. In the case of instruments with software digital data processing, the key role in the measurement channels is played by software algorithms, which largely determine their properties and the quality of the measurement process. Virtual instruments are also created in this way.

The aim of the research related to the content of this paper was to develop, calibrate and test the properties of a multi-channel temperature measurement system dedicated to research on energy dissipation from power cables in casing pipes with various fillers running in underground ducts [2]. Comparative temperature measurements were used to assess the efficiency of heat removal from the cable to surrounding media with different thermal properties. Predicted temperatures under these conditions usually range from

10 to 70 °C. In the form of a laboratory model simulating underground power lines, a test stand was developed for the experimental assessment of temperature distribution in casing pipes filled with various media surrounding the power cable [2]. A multi-channel temperature measurement system was required to perform the assessment as intended. The considered system consists of ten temperature measurement channels, but the number of measurement channels in the system is easy to expand.

Electricity is distributed worldwide mainly via overhead lines and increasingly using underground power cables [3–6]. Since the transmission of electricity is associated with the release of heat in the power line, an important issue affecting the permissible current carrying capacity (ampacity) of the cable used is a way of removing heat from the power cable, especially in the underground line [7–9]. Heat dissipation from underground cables has been analyzed in many publications in the form of numerical simulations [10–12] or on the basis of the results of experimental studies [13–15]. In all of them, the temperature distribution in the medium surrounding the power cable is an indicator of the efficiency of heat dissipation from the cable, buried directly in the ground or placed in casing pipes buried underground. The heat generation in the cable is due to the conductor resistance and the dielectric properties of the protective insulation of the cable. This heat has to be removed to the surrounding medium to avoid overheating of the cable insulation. The efficiency of heat dissipation depends on the properties of the surrounding medium, i.e., its thermal conductivity.

Temperature measurements are the most frequently performed measurements in industrial applications [16–19]. In digital instruments, temperature as a non-electrical analog quantity must first be converted by a suitable sensor into an electrical quantity and then by an ADC converter into its digital representation. The selection of temperature sensors with optimal properties from the point of view of the measurement system configuration is one of the important points related to the design of such a system. The following four most popular types of contact temperature sensors are used in continuous measurements in industrial applications [20,21]:

- Resistance temperature detectors (RTDs);
- Thermocouples;
- Semiconductor-based sensors;
- Negative temperature coefficient (NTC) thermistors.

RTD resistance increases with increasing temperature [22]. The RTD consists of a foil or a wire wrapped around a ceramic or glass core. Platinum sensors are the most accurate RTD sensors, while nickel and copper provide a lower cost; however, nickel and copper are not as stable and reproducible as platinum. Platinum RTDs offer highly accurate quasi-linear characteristics in the range of −200–850 °C but are significantly more expensive than copper or nickel.

A thermocouple consists of two electrically connected wires made of different metals' alloys [23]. The voltage generated between the two dissimilar metals changes with the temperature difference between the shorted and loose ends of the thermocouple. To specify the measured temperature, the reference temperature should be known. Thermocouples are non-linear sensors, and their accuracy is low, from 0.5 to 5 °C, but thermocouples operate over the widest temperature range, from −200 to 1750 °C.

A semiconductor-based temperature sensor is typically embedded in integrated circuits (ICs) [21,24]. These sensors use two identical diodes with temperature-sensitive voltage and current characteristics to monitor temperature changes. They offer a linear response but have the lowest accuracy of the basic sensor types. These temperature sensors also have the slowest response over the entire temperature range (−70–150 °C).

A thermistor Is a temperature-sensitive resistor that shows a continuous change in resistance that correlates with changes in temperature. NTC thermistor provides higher resistance at low temperatures [25–27] As the temperature rises, the resistance decreases. Small changes in temperature are reflected in large changes in resistance compared to other resistance temperature sensors. The characteristics of the NTC thermistor are non-linear

due to its exponential nature. The effective operating range is −50–150 °C for standard thermistors or up to 250 °C for glass thermistors.

PTC thermistors are also used in the measurement and control systems. These types of thermistors are divided into two groups depending on the materials used, their construction, and the production process. The first group of PTC thermistors consists of silistors that use silicon as a semiconductor material. They are used as PTC temperature sensors due to their linear resistance versus temperature characteristics, with a relatively slight slope over most of their operating range. Their temperature coefficients of resistance are much lower than the absolute values of these coefficients for NTC thermistors (negative). The second group is the switching type PTC thermistor. This type of thermistor has a highly non-linear temperature-resistance curve. When the switching type PTC thermistor is heated, the resistance first begins to decrease until it reaches a certain critical temperature. As the temperature continues to rise above this critical value, the resistance increases dramatically. These types of PTC thermistors are widely used in PTC heaters, threshold sensors, etc. Polymer PTC thermistors belong to the latter group and are often used as resettable fuses.

In this study, NTC thermistors were selected to measure the temperature in the channels of the developed system due to the advantages of using this type of sensor, e.g., small size and low cost, fast temperature response, high sensitivity, suitability for precise temperature measurement and control, and simple application circuits. At the same time, due to material and manufacturing criteria, standardization of semiconductor components such as NTC thermistors is difficult. Therefore, the possibilities of their interchangeable use are limited [28]. The temperature measurements with NTC sensors can be largely inaccurate for a variety of reasons. The most important of them are low stability (especially long-term) and low repeatability of the static characteristics of individual elements within a given type [28,29], resulting in poor interchangeability of these sensors in measurement devices [26].

In temperature measurement with thermocouples, in a wide range of applications, an accuracy of ±0.5–±2 °C is easily achievable, depending on the type of thermocouple and tolerance class [17,18,23].

With platinum RTDs, the temperature can be measured extremely accurately due to the stability of the material and the quasi-linear relationship between temperature and resistivity, and an accuracy of ±0.01–±0.3 °C can be easily achieved in industrial applications.

In [22] it is stated that the accuracy tolerance standard for the available RTDs ranges from 0.08 to 0.67 C depending on the RTD tolerance class and application circuit configuration. In [20], the accuracy of the platinum RTD thermometer is disclosed to be 0.3–4.6 °C.

The accuracy of typical semiconductor temperature sensors is within 0.5–4 °C [21]. Precision analog temperature sensors achieve an accuracy of 0.1–0.4 °C [24].

In paper [26], the accuracy of temperature measurement devices with an NTC thermistor calibrated by various methods is from 0.8 to 1.6 °C, while using the parameter values provided by the manufacturer, the inaccuracy exceeds 6 °C.

In all cases, the overall measurement accuracy is also affected by additional factors related to the properties of the sensor application circuits and other characteristics of the measurement system. The digital measurement system is usually supported by a controller enabling centralized data processing. Typically, temperature-measuring instruments using NTC sensors are based on microcontroller devices [30,31]. The actual course of non-linear characteristics is usually reproduced in the measurement algorithm using the Look-Up-Table method. Determining the actual sensor characteristics in connection with recalibrating or replacing the sensor and updating it in the thermistor software model is quite troublesome.

Multi-channel temperature measurements are performed in many applications [32–36]. Some of these systems were created as virtual instruments in the NI LabVIEW (National Instruments, Austin, TX, USA) environment [35,36]. NTC thermistors as temperature sensors are also used in multi-channel systems, although not very often [37,38]. They are usually connected to complex application circuits that are the inputs of measurement channels.

Paper [30] presents a temperature-measuring device using an NTC thermistor and is based on a microcontroller. Its measurement inaccuracy compared to a digital thermometer is over 3 °C.

In a multi-channel temperature sensor system [32] using semiconductor temperature sensors with a sensor output providing a pulse-width modulation (PWM) signal, the measurement errors ranged from −0.9 to +1.1 °C.

In the case of a multi-channel data measurement system containing temperature measurement channels with digital sensors [34], the absolute accuracy of any of the channels is estimated at ±0.2 °C when the manufacturer declares the accuracy of the digital sensor to be ±0.5 °C.

The recorder with NTC thermistors in a matrix of temperature sensors, controlled by a microprocessor with an ADC converter, is presented in [37]. The temperature measurement error is 1 °C. On the other hand, in [38], a multi-channel temperature measurement system consisting of a 16-channel multiplexer, 12-bit analog-to-digital converter, differential amplifier and NTC temperature sensors was described. Declared accuracy in temperature measurements is better than 0.1 °C.

The multi-channel temperature measurement system presented in this article, is a virtual instrument developed for measuring and registering the temperature distribution at specific points in the laboratory model of the underground power line. Virtual instrument [39] means a fully functional measuring instrument (or system) in which basic functions performed in hardware in traditional measurement circuits, such as correction of processing characteristics or mathematical operations on signals, have been transferred to software and are digital data operations implemented in software procedures.

The developed instrument is supported by the NI PXI platform, the NI LabVIEW environment, and NTC thermistors in the input circuits of the measurement paths. The measurement channels use the NI DAQ card installed in the NI PXI platform housing.

Built-in measurement channel calibration procedures are an important part of the system's functionality. Calibration results saved in files are used to determine and update the actual characteristics of individual temperature measurement channels.

Successfully completed tests of the developed device confirmed the validity of the assumptions regarding the following:

- Simple thermistor application circuits;
- The possibility of calibrating the measuring circuits within the implemented hardware and software configuration, using only an additional device for setting the temperature and a reference thermometer;
- No need to adjust elements and characteristics in the analog part of the measurement channels;
- Acceptable accuracy of temperature measurement in all channels,
- Satisfactory convergence of the obtained processing characteristics in individual channels.

The main theoretical contribution made to the empirical research is the development of a mathematical model of the measuring channel, taking into account the properties of linear and non-linear elements in the measuring channel, which is the starting point for the correct configuration of all software procedures performed in the developed device.

The article is organized as follows. In Section 2, following an overall system concept, details of the temperature sensors used, sensor application circuits, ADC operations, and data processing software were provided. Section 3 contains an explanation of the methodology for measuring channel calibration and examples of calibration results. The results of the measurements verifying the operation of the measurement channels are presented in Section 4. The last two parts of the article contain comments on the obtained results and conclusions summarizing the research on the developed multi-channel temperature measurement system.

2. Materials and Methods Used in the Development of a Multi-Channel Temperature Measurement System

Basic operations in all measurement channels in the developed virtual instrument are performed in software on digital data. Its configuration is shown in Figure 1. The instrument is based on the NI PXI measurement platform ***1*** with a user interface (screen, keyboard, and mouse) and NI terminal block ***2*** cooperating with a set of thermistors. The temperature information is obtained from the thermistors and is further processed in the NI LabVIEW environment. A temperature calibrator ***3*** (T-704 Mors, Gdynia, Poland) was applied to set specific temperatures during the calibration of measurement channels and during the testing of their properties. The digital temperature meter ***4*** (DT-34 [40]) was used as a reference instrument to verify the temperature setting.

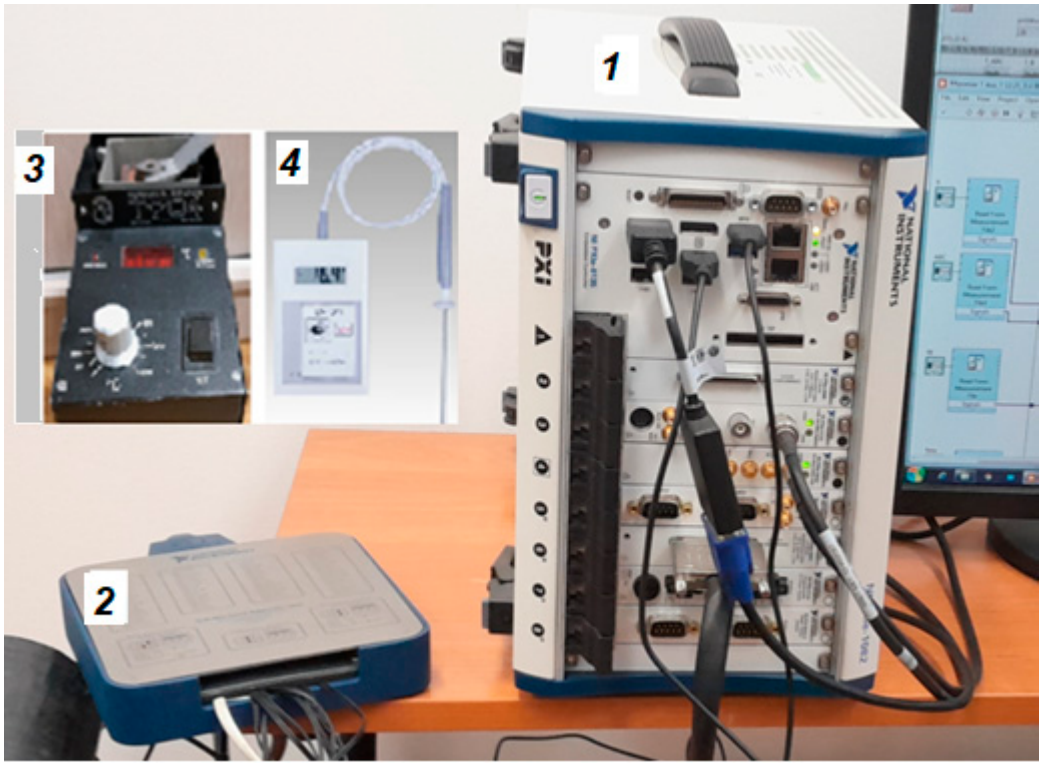

Figure 1. Developed multi-channel instrument and components for testing and calibration: ***1***—NI PXI measurement platform with NI DAQ card, ***2***—NI terminal block, ***3***—temperature calibrator, ***4***—digital thermometer.

A single temperature sensing circuit uses an additional resistor R_i (Figure 2) connected in series with the NTC thermistor R_{Ti}, which forms a thermistor conditioning circuit as a voltage divider, whose output voltage is fed to the input of the NI DAQ card installed in the NI PXI measurement platform. For all measurement channels, the additional resistors R_i are placed on the PCB (Printed Circuit Board) in the NI terminal block ***2*** (Figure 1). NTC thermistors, located on the measured object, have cable connections to their conditioning circuits. The eleven input channels of the NI DAQ card (Figure 2a) are used for measurements in the studies mentioned in the Introduction. Channel 0 (ch_0) is used to measure the voltage U_z, supplying the thermistor conditioning circuits, and another ten channels (ch_1—ch_10) are used to measure the output voltages U_i from voltage dividers. Figure 2b shows the thermistor cables connected to the pins on the NI terminal block.

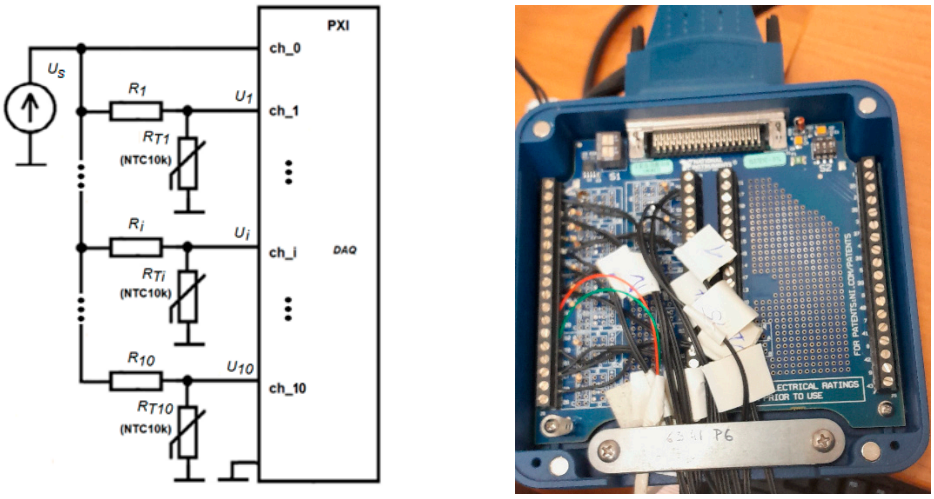

(**a**) (**b**)

Figure 2. Thermistor application circuits (**a**) and view of the thermistors wiring in the NI terminal block (**b**).

2.1. Measurement Platform

NI PXI measurement platform ***1*** (Figure 1) consists of the NI PXIe-1082Q (National Instruments Chassis) housing, which is equipped with the NI PXIe-8135 (Embedded Controller) and NI PXIe-6341 (DAQ card). The NI SH68M-68F-EPM cable (68-pin male VHDCI to 68-pin female D-SUB connector) connects the NI terminal block **2** to the DAQ card.

The NI PXIe-1082Q is an 8-Slot (4 hybrid slots, 2 PXIe Slots, 1 PXIe System Timing Slot) NI PXI Chassis [41].

The NI PXIe-8135 is an embedded Quad-Core 2.3 GHz (Intel Core i7) controller for NI PXI Express systems [42].

The NI PXIe-6341 DAQ card [43] includes, among others, 16 analog inputs (16-Bit, 500 kS/s), 2 analog outputs, 24 digital I/O, and four 32-bit counter/timers for PWM. The DAQ input channels in the developed system were configured in the NI terminal block [44] to operate in the RSE (Referenced Single-Ended) mode.

2.2. Terminal Block

The NI SCB-68A terminal block [44] provides a shielded I/O connection for interfacing I/O signals to a plug-in data acquisition device (DAQ card) with a 68-pin connector. The NI terminal block **2** (Figures 1 and 2b) is used for the acquisition of measurement data from all active channels. The voltage dividers (Figure 2a) form the R_{Ti} thermistor conditioning circuits in the individual channels and are mounted on the PCB inside the NI terminal block, adapted to the assembly of additional elements. The R_i resistors in each measuring channel i perform an auxiliary function, ensuring that the DAQ input voltages U_i change with changes of each resistance R_{Ti} according to the following relationship:

$$U_i = U_s \frac{R_{Ti}}{R_{Ti} + R_i} \tag{1}$$

where: U_s—the common supply voltage for all ten voltage dividers; i—number of specific channels (from 1 to 10); R_i—additional resistance in the voltage divider in channel i; R_{Ti}—resistance of thermistor in channel i.

The supply voltage U_s comes from the DAQ card and is obtained from 5 V through a series-connected 10 Ω resistor. The load is a parallel connection of ten voltage dividers with a resistance of several kΩ. It is a stable system due to the nature of temperature changes and therefore changes in the resistance of the thermistors.

2.3. Temperature Sensors

For linear or linearized elements, the mathematical description of the static characteristic using a linear function is unambiguous, while different non-linear models are used to describe the course of the NTC thermistor characteristics [25,45,46]. Basic mathematical models describing the non-linear relationship between thermistor resistance and temperature are created in one of the following two ways: using the Steinhart–Hart (S-H) equation or an equation with the material constant β (beta) [47,48].

The Steinhart–Hart equation takes the following form:

$$\frac{1}{T} = A + B \cdot lnR_T + C(lnR_T)^3 \tag{2}$$

where: T—temperature (in Kelvin [K] and T_C [°C] = T [K] − 273.15); R_T—resistance [Ω] of the sensor at temperature T [K]; A, B, C—coefficients with values dependent on the thermistor properties, possible to be determined in reference measurements.

The equation with the characteristic constant β of the NTC material, more commonly used by thermistor manufacturers to describe the course of the characteristics of thermistors, has the following form:

$$\frac{1}{T} = \frac{1}{T_0} + \frac{1}{\beta} \cdot ln\frac{R_T}{R_{T0}} \tag{3}$$

where: R_{T0}—sensor resistance [Ω] at temperature T_0 [K]; β [K]—material constant of the sensor.

The value of β is dependent upon material and thermistor construction and is considered unique for each thermistor.

Since the results obtained in verification measurements of the elaborated system using both thermistor models differ in practice to a lesser extent than the assumed measurement error, the article presents only the results obtained using the thermistor model with material constant β. It should be noted that software algorithms based on the Steinhart–Hart model are only slightly more complex, but they are as easy to implement in software as those referring to the model with the material constant β.

NTC10k thermistors, hermetic miniature sensors with a resistance of 10 kΩ at a temperature of 25 °C, were used as temperature sensors in the developed measuring system. The manufacturer of the NTC10k thermistors under consideration declares in the datasheet [49] that the sensor R_T resistance at 25 °C is 10 kΩ ± 1%, and its coefficient β is 3380 K ± 1%. The error area resulting from the permissible dispersion of these parameters, using Formula (3) to determine the temperature, is shown in Figure 3. The combination of the permissible deviations of the thermistor resistance and the material constant β, according to the manufacturer's data, creates a plane of permissible errors in determining the temperature with the thermistor in the given temperature range. This means that for temperatures in the range of 0–100 °C, the temperatures determined by individual sensors may differ from the actual temperature by the value of ΔT, located in the area limited by colored lines in Figure 3. These considerations do not take into account other factors contributing to measurement errors.

As mentioned earlier, the fabrication of thermistors is associated with low repeatability of the static characteristics of individual elements within a given type. Subsequent thermistors on the production line can differ in parameters in the mathematical model describing their properties. In order to use the thermistor mathematical model to measure temperature with greater accuracy than can be obtained based on the accuracy declared by the thermistor manufacturer, it is necessary to perform a reference measurement cycle at several temperatures to determine the sensor resistance values at these temperatures. Then, the values of the appropriate coefficients appearing in the mathematical formulas describing the static properties of individual thermistors can be calculated. To increase the accuracy of temperature measurement with the use of selected NTCs in the developed device, each measurement channel should be calibrated in terms of determining the properties of each thermistor and its application circuit at the DAQ input. In other words, the

parameters of the static characteristics of each thermistor and the resistances of the auxiliary resistors in each of the voltage dividers should be determined.

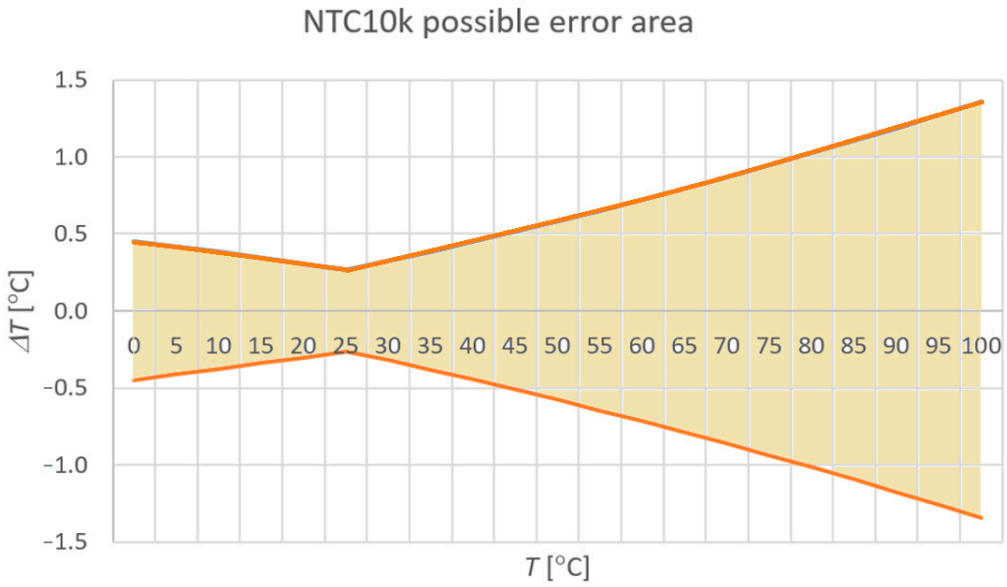

Figure 3. Temperature measurement error area (in yellow) related to NTC thermistors used in measurement channels.

2.4. Software Procedures in a Virtual Instrument

Software procedures are an integral part of the measurement channels. These procedures process the data provided by the DAQ card. In turn, DAQ inputs collect analog signals from individual temperature measurement channels, including NTC sensors in their conditioning circuits. These procedures also include several additional operations, including calibration of each of the measurement channels and verification of their processing characteristics, in particular, the following:

- Determination of the value of auxiliary resistors R_i in the input circuits of every channel (Figure 2a);
- Measurements of resistance R_{Ti} of thermistors at selected temperatures;
- On the basis of the two previous steps, the determination of coefficient values in the mathematical model for individual thermistors;
- Temperature verification measurements using designated models for individual thermistors and for entire measurement channels.

The basic procedures performed as a part of the operation of the measurement system are shown in Figure 4. Dashed lines show the data flow between procedures.

The purpose of the procedure ① (Figure 4) is to determine the value of the auxiliary resistors R_i in individual voltage dividers (Figure 2). These values are used in both other procedures.

The calibration procedure of measuring channels ② (Figure 4) is used for determining coefficients in a mathematical model of individual measurement channels based on the determined thermistor resistances at specified temperatures and the characteristics of individual voltage dividers. The results can be used in accuracy assessment [27,34].

The multi-channel temperature measurement procedure ③ is the target procedure of the instrument. Temperature measurements are made continuously in subsequent cycles, and the results are stored in the system's memory.

The "User Action" header operation allows the operator to move between procedures and activate the selected one.

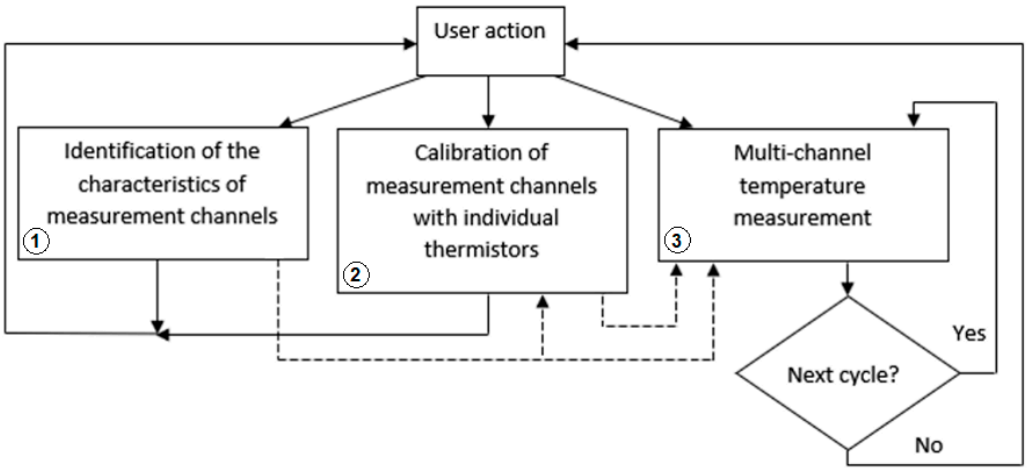

Figure 4. Block diagram of calibration and measurement procedures.

3. Identification of Characteristics and Calibration of Measurement Channels

Determination of the processing characteristics of individual measurement channels of the developed instrument is carried out with the use of additional elements as follows: a reference resistor R_{ref} and a vessel with a mixture of water and ice.

Identification of the actual characteristics of individual channels (procedure ① in Figure 4) requires determining the value of auxiliary resistors R_i in individual voltage dividers (Figure 2a). Calibration of the measurement path (procedure ② in Figure 4) consists in determining the coefficients in a mathematical model representing the characteristics of a given thermistor.

3.1. Determination of the Value of Auxiliary Resistors R_i in Voltage Dividers

The U_i voltages from individual channels equipped with voltage dividers and the supply voltage U_s, delivered to the inputs of the DAQ (Figure 2), are converted there into their digital representations. Assuming that the input resistance of the DAQ channel (here: 10 GΩ [43]) is much greater than the resistances used in the voltage divider, the Equation (1) is used to determine the output voltage U_i of the voltage divider.

To determine how the resistance R_{Ti} is converted to the output voltage U_i, it is necessary to know the exact value of the resistance R_i of the auxiliary resistor in the voltage divider. The values of the R_i resistances were initially selected at approx. 5 kΩ in order to obtain high measurement sensitivity in the temperature range, which is important from the point of view of the measurement application. The actual values of the resistances R_i, installed in the individual circuits, were determined using a reference resistor R_{ref} with a resistance of 5001 Ω and accuracy class index 0.05% (with expanded uncertainty equal to 2.8 Ω at the confidence level of approx. 95%). During measurements, this resistor was connected sequentially in place of the individual thermistors R_{Ti} (Figure 2a). For each channel i, the value of auxiliary resistance R_i can be calculated using the following formula:

$$R_i = R_{ref}\frac{U_s - U_i}{U_i} \tag{4}$$

The software routine in LabVIEW calculates the required values and stores the results in a semi-automatic cycle in response to the user's command. In Table 1, the values of the R_i auxiliary resistors determined for ten measurement channels are shown. They were calculated in software as averaged resistances determined from the series of 30 voltage results and from Formula (4) and presented together with standard deviations resulting from the dispersion of the results in each series. It was assumed that the measurement series consisting of 30 samples was large enough to determine the average value, of which would not differ significantly from the average value calculated on the basis of the results in the measurement series with a larger number of samples. The number of samples can be

easily changed in the algorithms of the virtual instrument, which involves changing the volume of the recorded data files.

Table 1. The R_i auxiliary resistors with the corresponding standard deviations (*sd*).

	ch_1	**ch_2**	**ch_3**	**ch_4**	**ch_5**	**ch_6**	**ch_7**	**ch_8**	**ch_9**	**ch_10**
R_i [Ω]	5010.84	5039.60	4967.59	5042.50	4984.41	4960.30	4985.02	4982.53	4993.29	5026.93
sd [Ω]	2.02	2.97	2.06	2.29	2.38	2.90	2.00	2.26	2.37	2.72

The obtained accuracy of the determined resistances R_i can be compared to highly accurate resistors with an accuracy class of 0.05% and precise resistors with better accuracy are expensive on sale.

3.2. Determination of R_{Ti} Resistance Values of Thermistors at Specific Temperatures

Analogously to the determination of the resistances R_i (Figure 2a) and using previously calculated R_i values for individual channels (Table 1), the measurement of R_{Ti} values at specific temperatures is based on the processing of digital representations of input voltages in channels 0–10 of the DAQ card (Figure 2a).

The measurement was performed for temperatures T_r equal to 0 °C and about 100 °C. The selection of temperatures is related to the intended measuring range of the developed instrument.

Data collected for these temperatures were saved in separate files (both in *.xlsx* and *.lvm* format).

The samples of averaged voltages with the corresponding standard deviations related to channel 1, used to determine the R_{T1} values corresponding to the actual temperature points, are shown in Table 2.

Table 2. The averaged voltages with corresponding standard deviations (*sd*): (**a**) U_s in ch_0 and (**b**) U_{T1} in ch_1 as an example.

(a)			**(b)**		
T_r [°C]	U_s [V]	*sd* [V]	T_r [°C]	U_{T1} [V]	*sd* [V]
0.0	4.97149	0.00007	0.0	4.20782	0.00008
99.3	4.90314	0.00010	99.3	0.82266	0.00036

After measuring the voltages in eleven DAQ channels, and then using the Formula (4) and the value of the resistance R_i in individual channels (Table 1), it is possible to calculate the resistance R_{Ti} at the corresponding temperatures T_r as follows:

$$R_{Ti} = R_i \frac{U_{Ti}}{U_s - U_{Ti}} \tag{5}$$

In Table 3, the values of R_{Ti} resistances of the thermistors on the inputs of channels 1–10 are shown. They have been calculated as averaged resistances derived from a series of ADC conversions of each voltage and using Formula (5).

Table 3. The values of R_{Ti} resistances of the thermistors in channels 1–10 determined at specific temperatures.

T_r [°C]		**ch_1**	**ch_2**	**ch_3**	**ch_4**	**ch_5**	**ch_6**	**ch_7**	**ch_8**	**ch_9**	**ch_10**
0.00	R_{Ti} [Ω]	27,609.7	27,316.5	27,456.3	27,569.3	27,586.0	27,589.5	27,501.9	27,472.8	27,360.5	27,372.9
99.3		1010.2	1001.3	1004.2	1016.6	1008.3	1005.5	1005.1	1005.5	990.9	991.7

3.3. Calculation of Coefficient Values in the Equation Approximating the Characteristics of Thermistors

Knowing the resistance values of the thermistors, corresponding to individual temperature points, it is possible to determine the values of the coefficients in models describing the characteristics of temperature-to-resistance conversion for individual thermistors. The procedures related to Equations (2) or (3) use the same sets of previously collected data on specific temperatures T_r and corresponding resistances R_{Ti}. For each of the 10 thermistors, the corresponding data can be used to calculate the coefficients appearing in Formula (2) (here: three reference temperature points are needed) and Formula (3), respectively, although, as was mentioned previously, in this paper the derivation of the relationship for determining the coefficients in Equation (3) will be shown.

The values of the β_I coefficients were determined for all 10 thermistors based on the calculated values R_{T1i} and R_{T2i}, obtained for the temperature points 0 °C ($T_r = T_1$) and 99.3 °C ($T_r = T_2$) (Table 3), using the formula obtained from Equation (3) as follows:

$$\beta_I = ln(\frac{R_{T2i}}{R_{T1i}}) \frac{1}{\left(\frac{1}{T_2} - \frac{1}{T_1}\right)} \tag{6}$$

where: for specific channel i, the values of T_0 and R_{T0} in Equation (3) correspond to the values T_1 and R_{T1i} in Equation (6), respectively.

The values of individual β_i coefficients for ten channels are shown in Table 4.

Table 4. The values of β_i coefficients of sensors in individual channels.

	ch_1	**ch_2**	**ch_3**	**ch_4**	**ch_5**	**ch_6**	**ch_7**	**ch_8**	**ch_9**	**ch_10**
β_i [K]	3389.1	3387.2	3389.5	3381.2	3390.1	3393.1	3390.3	3388.8	3399.5	3399.2

The values of the β_i coefficients for all thermistors are within the accuracy range specified by the manufacturer of the thermistors used in the test (3346.2–3413.8 K). The maximum deviation of the actual values of the determined coefficients from the nominal value (3380 K) is about 0.58%.

4. The Results of the Verification Measurements

In the developed measurement system, the same channels used to identify the characteristics of thermistors were used as measurement channels. The mathematical model of the measuring channel i, in the system shown in Figure 2a, takes into account the conversion of the temperature T_i into the resistance R_{Ti} and then the R_{Ti} into the voltage U_i being the input voltage of the ADC, and finally, the voltage U_i is converted in the ADC to its digital representation D_i. For individual channels, the mathematical model $D_i = f(T_i)$ describes the way of processing information in the acquisition part of the channel. For the system under consideration, the conversion of T_i into D_i is described as the sequence of conversions as follows:

$$R_{Ti} = f(T_i) \text{ then } U_i = f(R_{Ti}, R_i, U_s) \text{ and } D_i = f(U_i);\ D_s = f(U_s) \tag{7}$$

where: R_i is the auxiliary resistance in channel i; U_s is the measured supply voltage; U_i is the input voltage of the ADC in channel i; D_i and D_s are the digital representations of input voltages U_i and U_s, and R_{Ti}, as a function of T_i, is the resistance determined on the basis of the transformed dependency (3), which is the individual thermistors approximation characteristics with corresponding coefficients determined in the previous section.

Since the digital DAQ output data is automatically converted in the LabVIEW environment to DAQ input voltage units, the characteristics of the ADC converter can be described as follows:

$$D_i = U_i;\ D_s = U_s \tag{8}$$

The resistance R_{Ti} can be calculated using the following formula:

$$R_{Ti} = \frac{D_i \cdot R_i}{D_s - D_i} \tag{9}$$

In order to perform the software determination of T_i for individual channels in the temperature measurement procedure ③ (Figure 4), the calculated values of R_{Ti} should be included in the Equation (3) together with the following previously determined other factors: T_0, R_{T0i}, and β_i. The mathematical model obtained in this way to determine the temperature T_i is implemented as a software part of individual measurement channels and is the subject of experimental research.

The results of the verification measurements, containing the average temperatures (T_A) calculated from the temperatures obtained in all 10 channels, in relation to the corresponding reference temperatures T_{ref}, are presented in Table 5. Reference temperatures T_{ref} were measured with a DT-35 digital thermometer [40].

Table 5. The measurement results of T_A temperatures averaged from 10 sensors in relation the reference temperatures T_{ref}.

T_{ref} [°C]	23.3	29.1	40.1	50.6	59.8	69.8	79.1	88.4	100.2
T_A [°C]	23.27	29.04	39.99	50.57	59.73	69.75	79.00	88.40	100.30

In Table 6, the differences between the temperatures obtained from exemplary channel 1 (ch_1) and the reference temperatures (T_{ref}) are shown in relation to the reference temperatures (T_{ref}).

Table 6. The differences between the temperatures (T_1) and the reference temperatures (T_{ref}) (data for channel 1).

T_{ref} [°C]	23.3	29.1	40.1	50.6	59.8	69.8	79.1	88.4	100.2
$T_1 - T_{ref}$ [°C]	0.04	0.00	0.06	0.00	0.05	0.04	0.16	0.21	0.31

Figure 5, on the example of the results from channel 1, shows the differences between the temperatures determined from the Formula (3) and the reference temperatures (T_{ref}) in relation to T_{ref}. Additionally, standard deviations resulting from the dispersion of the results in the series in each of the measurement points for this channel have been marked. The results obtained for the other channels were similar.

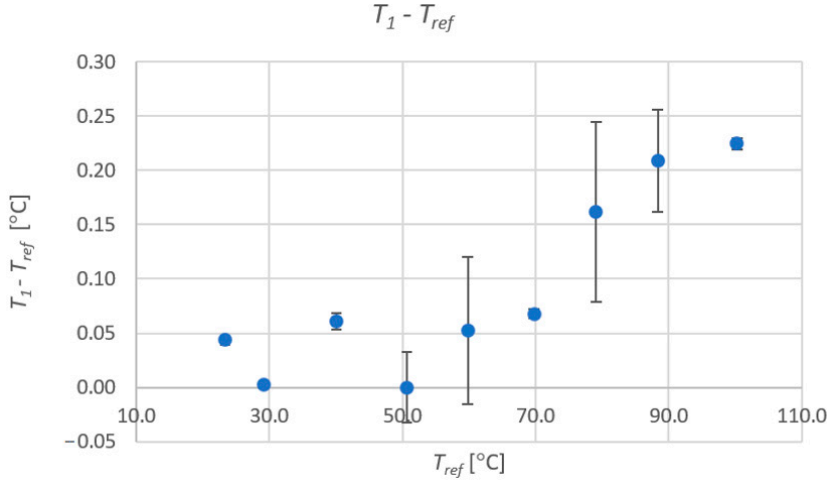

Figure 5. The differences between the temperatures determined in ch_1 and the reference temperatures (T_{ref}), in relation to T_{ref}.

Figure 6 contains a graph of the differences between the temperatures obtained in verification tests for all ten channels and the reference temperatures (T_{ref}), in relation to the reference temperatures. It shows the course of residual errors, defined as differences between temperatures determined in measurement channels, taking into account mathematical models describing the characteristics of individual sensors and temperature reference data.

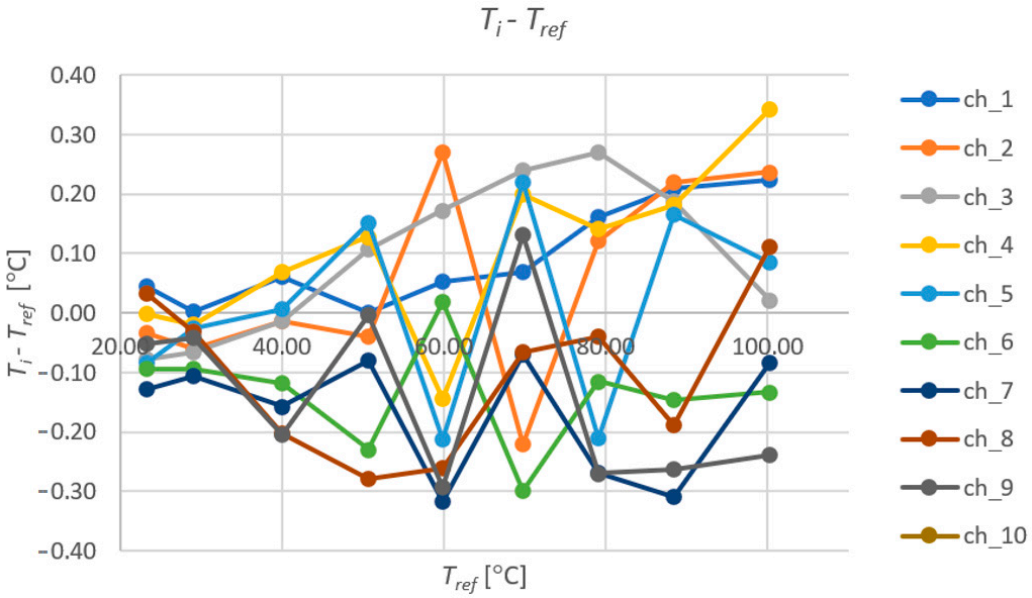

Figure 6. The course of differences between the temperatures determined in ten channels and the reference temperatures in relation to the reference temperatures (T_{ref}).

5. Discussion

The satisfactory accuracy of the temperature measurement results obtained with the developed instrument, confirmed during verification tests, depends on the appropriate configuration of the acquisition part of measurement channels and on the correctness of subsequent procedures leading to the determination of the characteristics of individual channels, including the identification of coefficients in mathematical models of individual NTC thermistors. During the verification measurements, the satisfactory convergence of the obtained processing characteristics in individual channels was confirmed.

The systemic configuration of measurement channels is simpler than in similar temperature measuring instruments, e.g., described in [35,36,38]. The use of the NI PXI platform together with the NI DAQ card in the developed device allowed for a simple configuration of the thermistor application circuits ensuring the correct acquisition of temperature information. Thanks to this, it was possible to transfer to the software the implementation of complex functions, including non-linear ones, which must be performed for the correctness of measurements and are incomparably easier to perform in software procedures than in analog circuits.

As part of the implemented hardware and software configuration of the device, the calibration of the measurement channels is carried out only with the use of an additional device for setting the temperature and a reference thermometer. It is not necessary to determine the characteristics of the sensors using external measuring systems, e.g., as in [26,38]. In the acquisition part of the measurement channels, there are no elements that require adjustment during calibration in order to obtain the desired processing properties.

The quality of determination of characteristics of the measuring path depends largely on the accuracy of the stabilization of the reference temperatures during the calibration procedures of the track elements. Since the resolution of the NI DAQ card [43] used in the system and its accuracy, as well as the procedures for programming the measurement paths have been verified in numerous tests, the main emphasis in the calibration procedures of

the measurement system should be on precise temperature stabilization and ensuring good thermal coupling of all sensors in the temperature calibrator. Residual errors observed as variations in the temperature error curves in the measurement channels (Figure 6) may be the result of temperature differences in the thermal calibrator chamber in which the tested sensors were located together, both at the stage of identifying the processing characteristics in individual channels and during verification measurements. The level of these errors is quite low compared to the results of other studies, e.g., described in [26].

The operations related to the developed device were performed in the presence of various random disturbances, the effects of which were observed as different sample values in the measurement series, with the measurement conditions unchanged. The impact of accompanying factors on the obtained results was effectively reduced by acquiring a series of measurements instead of simple samples at each stage of the research.

Compared with other solutions of multi-channel devices operating on the basis of invasive contact methods of temperature measurement, shown for example in [16–24], several properties of the method used can be indicated. In addition to the positive features, such as the high measurement sensitivity of NTC thermistors and the simplicity of analog application circuits, determining the temperature value in each of the measurement channels requires performing calculations using non-linear functions, taking into account individual parameter values in each of the channels. In addition, unlike other types of sensors, each replacement of the NTC thermistor with a different one must be accompanied by the introduction of its current parameters to the measurement algorithms. Their determination is possible as a result of performing an additional operation, shown in Figure 4, as procedure 2 built into the developed software of the device.

6. Conclusions

The adopted configuration of the measurement channels turned out to be correct, taking into account that the assumed accuracy for each channel has been achieved not worse than ± 0.4 °C. This accuracy is sufficient due to the needs related to the implementation of the system in conducted research on heat dissipation from the underground power cable routed in a casing pipe. It can be easily increased by performing more precise calibration procedures under the control of software routines included in the developed instrument and by improving the reference temperatures' stabilization system.

One of the advantages of the developed configuration of the multi-channel temperature measurement system is the simplicity of the hardware part of the measurement channels. All procedures related to the identification of the properties of individual channels and measurement operations are performed by software. There is no need to adjust any hardware components in the system. The implemented algorithms make it possible to perform calibration operations of all measurement channels along with updating the characteristics of thermistors at any time.

The article presents only a selected part of the results collected during system calibration and testing. In the conducted research, regardless of the algorithms for determining the thermistor characteristics based on the material constant β model, algorithms based on the Steinhart–Hart model were used. Two mathematical models of NTC thermistors, implemented during the experiments, faithfully reflect the characteristics of these sensors, and the quality of determining the coefficients present in these models obviously affects the accuracy of subsequent measurements. During the experiments, slight deviations between the temperature measurement results obtained on the basis of these two models of thermistor characteristics were observed. They did not exceed 0.2 °C in the entire measurement range, which, in relation to the accuracy requirements of the implemented temperature measurement system, indicates a sufficient accuracy of the determined thermistor characteristics based on each of these two models.

Author Contributions: Conceptualization. R.M. and D.S.; methodology. R.M. and D.S.; software. R.M.; validation. R.M. and D.S.; formal analysis. R.M.; investigation. R.M.; resources. R.M. and D.S.; data curation. R.M.; writing—original draft preparation. R.M.; writing—review and editing. R.M.; visualization. R.M.; supervision. D.S.; project administration. R.M. All authors have read and agreed to the published version of the manuscript.

Funding: This research received no external funding.

Data Availability Statement: The data presented in this study are openly available in numerous files in the "Bridge of Knowledge" ("Most wiedzy") repository at https://doi.org/10.34808/exdv-6t87 and in other related resources available in the referenced repository.

Conflicts of Interest: The authors declare no conflict of interest.

Abbreviations

ADC	Analog-to-Digital Converter
DAQ	Data Acquisition
IC	Integrated Circuit
LabVIEW	Laboratory Virtual Instrumentation Engineering Workbench
NI	National Instruments
NTC	Negative Temperature Coefficient
PCB	Printed Circuit Board
PCI	Peripheral Component Interconnect
PXI	PCI eXtensions for Instrumentation
PXIe	PXI Express
PTC	Positive Temperature Coefficient
RSE	Referenced Single-Ended
RTD	Resistance Temperature Detectors
SCB	Shielded I/O Connector Terminal Block
Symbols	
A, B, C	Coefficients with values dependent on the thermistor properties (Steinhart–Hart equation)
β (β_i)	Material constant of the thermistor (β equation) (in channel i)
D_i (D_s)	Digital representation of the ADC input voltage in channel i (supply voltage)
i	The number of the specific channel (from 1 to 10)
R_i	The resistance of the auxiliary resistor in the voltage divider in channel i
R_{ref}	Reference resistor to determine the resistance value of the resistors R_i
R_T	Resistance of the thermistor at temperature T
R_{T0}	Thermistor resistance [Ω] at temperature T_0
R_{Ti}	Resistance of the thermistor in channel i
sd	Standard deviation
T_A	Average temperature measurement result from 10 sensors
T (T_i)	Temperature (in channel i)
T_r (T_1, T_2)	Reference temperatures to determine the parameters of the thermistor
T_{ref}	Reference temperature measured with a digital thermometer during the instrument calibration procedure
U_i	The output voltage of the voltage divider in channel i; at the same time, the input voltage of the ADC in channel i
U_s	Common supply voltage for all ten voltage dividers
U_{Ti}	Corresponds to the voltage U_i when determining the value of R_{Ti} at the temperature T_r

References

1. Eren, H. Chapter 1.1—Analog vs. Digital Instruments. In *Instrumentation Engineers Handbook: Process Control and Optimization*, 4th ed.; CRC Press Taylor & Francis Group: Boca Raton, FL, USA, 2005; Volume 2, pp. 3–15.
2. Masnicki, R.; Mindykowski, J.; Palczynska, B. Experiment-Based Study of Heat Dissipation from the Power Cable in a Casing Pipe. *Energies* **2022**, *15*, 4518. [CrossRef]
3. Bascom, E.C.; Antoniello, V.D. Underground Power Cable Considerations: Alternatives to Overhead. In Proceedings of the 47th Minnesota Power Systems Conference (MIPSYCON), Brooklyn Center, MN, USA, 1–3 November 2011.
4. Orton, H. History of underground power cables. *IEEE Electr. Insul. Mag.* **2013**, *29*, 52–57. [CrossRef]

5. Hall, K.L. *Out of Sight, out of Mind. An Updated Study on the Undergrounding of Overhead Power Lines*; Edison Electric Institute: Washington, DC, USA, 2012.
6. Mueller, C.E.; Keil, S.I.; Bauer, C. Underground cables vs. overhead lines: Quasi-experimental evidence for the effects on public risk expectations, attitudes, and protest behavior. *Energy Policy* **2019**, *125*, 456–466. [CrossRef]
7. Metwally, I.A.; Al-Badi, A.H.; Al Farsi, A.S. Factors influencing ampacity and temperature of underground power cables. *Electr. Eng.* **2013**, *95*, 383–392. [CrossRef]
8. Maximov, S.; Venegas, V.; Guardado, J.L.; Moreno, E.L.; López, R. Analysis of underground cable ampacity considering non-uniform soil temperature distributions. *Electr. Power Syst. Res.* **2016**, *132*, 22–29. [CrossRef]
9. Bustamante, S.; Mínguez, R.; Arroyo, A.; Manana, M.; Laso, A.; Castro, P.; Martinez, R. Thermal behaviour of medium-voltage underground cables under high-load operating conditions. *Appl. Therm. Eng.* **2019**, *156*, 444–452. [CrossRef]
10. Quan, L.; Fu, C.; Si, W.; Yang, J.; Wang, Q. Numerical study of heat transfer in underground power cable system. *Energy Procedia* **2019**, *158*, 5317–5322. [CrossRef]
11. Ocłoń, P.; Cisek, P.; Pilarczyk, M.; Taler, D. Numerical simulation of heat dissipation processes in underground power cable system situated in thermal backfill and buried in a multilayered soil. *Energy Convers. Manag.* **2015**, *95*, 352–370.
12. Hruška, M.; Clauser, C.; De Doncker, R.W. Influence of dry ambient conditions on performance of underground medium-voltage DC cables. *Appl. Therm. Eng.* **2019**, *149*, 1419–1426. [CrossRef]
13. Verschaffel-Drefke, C.; Schedel, M.; Balzer, C.; Hinrichsen, V.; Sass, I. Heat Dissipation in Variable Underground Power Cable Beddings: Experiences from a Real Scale Field Experiment. *Energies* **2021**, *14*, 7189. [CrossRef]
14. Ocłoń, P.; Pobędza, J.; Walczak, P.; Cisek, P.; Vallati, A. Experimental validation of a heat transfer model in underground power cable systems. *Energies* **2020**, *13*, 1747. [CrossRef]
15. Ahmad, S.; Rizvi, Z.; Khan, M.A.; Ahmad, J.; Wuttke, F. Experimental study of thermal performance of the backfill material around underground power cable under steady and cyclic thermal loading. *Mater. Today Proc.* **2019**, *17*, 85–95. [CrossRef]
16. Childs, P.R.N.; Greenwood, J.R.; Long, C.A. Review of temperature measurement. Review article. *Rev. Sci. Instrum.* **2000**, *71*, 2959–2978. [CrossRef]
17. Ross-Pinnock, D.; Maropoulos, P.G. Review of industrial temperature measurement technologies and research priorities for the thermal characterisation of the factories of the future. *J. Eng. Manuf. Part B* **2016**, *230*, 793–806. [CrossRef]
18. Michalski, L.; Eckersdorf, K.; Kucharski, J.; McGhee, J. *Temperature Measurement*, 2nd ed.; John Wiley & Sons Ltd.: Chichester, UK, 2001.
19. Industrial Temperature Measurement. AMETEK Calibration Instruments. Available online: https://www.ametekcalibration.com/-/media/ametekcalibration/download_links/temperature-sensors/industrial-temperature-measurement-us.pdf?revision=2f3d457c-1381-4988-a2b7-333356e74912 (accessed on 10 January 2023).
20. Industrial Temperature Measurement. Basics and Practice. ABB Measurement & Analytics. Available online: https://library.e.abb.com/public/bc79d6844ab746809f1930b61656c791/03_TEMP_EN_E02.pdf (accessed on 10 January 2023).
21. National Semiconductor's Temperature Sensor Handbook. Available online: https://shrubbery.net/~heas/willem/PDF/NSC/temphb.pdf (accessed on 10 January 2023).
22. A Basic Guide to RTD Measurements. Texas Instruments. Application Report. Available online: https://www.ti.com/lit/an/sbaa275/sbaa275.pdf?ts=1674134106286&ref_url=https%253A%252F%252Fwww.google.com%252F (accessed on 10 January 2023).
23. A Basic Guide to Thermocouple Measurements. Texas Instruments. Application Report. Available online: https://www.ti.com/lit/an/sbaa274/sbaa274.pdf?ts=1673898633273&ref_url=https%253A%252F%252Fwww.google.com%252F (accessed on 10 January 2023).
24. LMT70, LMT70A ±0.05 °C Precision Analog Temperature Sensor. Texas Instruments. Available online: https://www.ti.com/lit/ds/snis187a/snis187a.pdf?ts=1674125205944&ref_url=https%253A%252F%252Fwww.google.com%252F (accessed on 10 January 2023).
25. Cong, Y.; Wang-Chao, Z.; Bin, S.; Hang-Xia, Z. Study on NTC Thermistor Characteristic Curve Fitting Methods. In Proceedings of the International Conference on Computer Science and Network Technology, Harbin, China, 24–26 December 2011; pp. 2209–2213.
26. Liu, Y.; Liu, Y.P.; Zhang, W.; Zhang, J. The Study of Temperature Calibration Method for NTC Thermistor. In Proceedings of the 2020 IEEE the 4th International Conference on Frontiers of Sensors Technologies, Shanghai, China, 6–9 November 2020; pp. 50–53.
27. Liu, G.; Guo, L.; Liu, C.; Wu, Q. Evaluation of different calibration equations for NTC thermistor applied to high-precision temperature measurement. *Measurement* **2018**, *120*, 21–27. [CrossRef]
28. Wood, S.D.; Mangum, B.W.; Filliben, J.; Tillett, S.B. An Investigation of the Stability of Thermistors. *J. Res. Natl. Bur. Stand.* **1978**, *83*, 247–263. [CrossRef]
29. Park, K. Improvement in electrical stability by addition of SiO_2 in $(Mn_{1.2}Ni_{0.78}Co_{0.87-x}Cu_{0.15}Six)O_4$ negative temperature coefficient thermistors. *Scr. Mater.* **2004**, *50*, 551–554. [CrossRef]
30. Munifah, S.S.; Aminudin, A. Design of temperature measuring instrument using NTC thermistor of Fe_2TiO_5 based on microcontroller aTmega 328. MSCEIS 2018. *J. Phys. Conf. Ser.* **2019**, *1280*, 022052. [CrossRef]
31. Panpan, Z.; Bifeng, Y.; Yi, Z.; Shangchang, M. A Multi-Channel Temperature Measurement and Fusion System Based on Cortex-M4. In Proceedings of the 2019 International Conference on Meteorology Observations (ICMO), Chengdu, China, 28–31 December 2019; pp. 1–4.

32. Kalas, D.; Pretl, S.; Reboun, J.; Soukup, R.; Hamacek, A. Towards Hand Model with Integrated Multichannel Sensor System for Thermal Testing of Protective Gloves. *Period. Polytech. Electr. Eng. Comput. Sci.* **2018**, *62*, 165–171. [CrossRef]
33. Zhang, Y.; Bai, X.; Zhan, J.; Zhang, Y. Multi-Channel and High-Reliability Temperature Acquisition System Based on RS422 and USB Bus. In Proceedings of the International Conference on Electronic & Mechanical Engineering and Information Technology, Harbin, China, 12 August 2011; pp. 1372–1375.
34. Yurkov, N.K.; Proshin, A.A.; Goryachev, N.V.; Grishko, A.K. Metrology Model of Measuring Channel in Multi-Channel Data-Measurement System. In Proceedings of the 2020 International Conference on Engineering Management of Communication and Technology (EMCTECH), Vienna, Austria, 20–22 October 2020; pp. 1–4.
35. Zhu, W.; Liu, J.; Yang, H.; Yan, C. Design of High Precision Temperature Measurement System based on LabVIEW. *Int. J. Adv. Comput. Sci. Appl.* **2015**, *6*, 153–155. [CrossRef]
36. Ren, J.; Liu, D.; Liu, W.; Wang, X. Multi-Channel Temperature Measurement System based on LabVIEW. *Int. J. Eng. Res. Technol.* **2015**, *4*, 485–488.
37. Lee, C.J.; Shie, M.C. A Temperature Sensor Array Recorder with Fast and Multi-Channel Measurements. In Proceedings of the IEEE International Conference on Signal Processing, Communication and Computing (ICSPCC), Kunming, China, 5–8 August 2013; pp. 1–4.
38. Eke, R.; Kavasoglu, S.A.; Kavasoglu, N. Design and implementation of a low-cost multi-channel temperature measurement system for photovoltaic modules. *Measurement* **2012**, *45*, 1499–1509. [CrossRef]
39. Virtual Instrumentation. National Instruments. Available online: https://www.ni.com/pl-pl/innovations/white-papers/06/virtual-instrumentation.html (accessed on 10 January 2023).
40. Industrial Calibrated Thermometer DT-34. Available online: https://termoprodukt.co.uk/calibrated-industrial-thermometer-dt-34?search=dt-34 (accessed on 10 August 2021).
41. PXIe-1082 Specifications. National Instruments. Available online: https://www.ni.com/docs/en-US/bundle/pxie-1082-specs/page/specs.html# (accessed on 10 January 2023).
42. NI PXIe-8135 User Manual. National Instruments. Available online: https://www.ni.com/docs/en-US/bundle/pxie-8135-seri/resource/373716b.pdf (accessed on 10 January 2023).
43. NI PXIe-6341 Specifications. National Instruments. Available online: https://www.ni.com/pdf/manuals/377881a.pdf (accessed on 10 January 2023).
44. NI SCB-68A User Manual. National Instruments. Available online: https://www.ni.com/docs/en-US/bundle/scb-68a-seri/resource/375865a.pdf (accessed on 10 January 2023).
45. Steinhart, J.S.; Hart, S.R. Calibration curves for thermistors. *Deep Sea Res. Oceanogr. Abstr.* **1968**, *15*, 497–503. [CrossRef]
46. Ilic, D.; Butorac, J.; Ferkovic, L. Temperature measurements by means of NTC resistors and a two-parameter approximation curve. *Measurement* **2008**, *41*, 294–299. [CrossRef]
47. Liu, G.; Guo, L.; Liu, C.; Wu, Q. Uncertainty propagation in the calibration equations for NTC thermistors. *Metrologia* **2018**, *55*, 437–445. [CrossRef]
48. Chen, C. Evaluation of resistance–temperature calibration equations for NTC thermistors. *Measurement* **2009**, *42*, 1103–1111. [CrossRef]
49. NTC Thermistor NTC10k–OKY3065-5. OKYSTAR. Available online: https://www.okystar.com/product-item/ntc-thermistor-ntc-10k-oky3065-5/ (accessed on 10 August 2021).